Rock Mech. Rock Engng. (2008) 41 (2), 299–323
DOI 10.1007/s00603-006-0115-6
Printed in The Netherlands

Rock Mechanics and Rock Engineering

Rock Joint Surfaces Measurement and Analysis of Aperture Distribution under Different Normal and Shear Loading using GIS

By

M. Sharifzadeh[1,2], **Y. Mitani**[2], and **T. Esaki**[2]

[1] Department of Mining, Metallurgy and Petroleum Engineering, Amirkabir University of Technology, Tehran, Iran
[2] Faculty of Engineering, Institute of Environmental Systems, Kyushu University, Kyushu, Japan

Received October 7, 2004; accepted July 7, 2006
Published online October 17, 2006

Summary

The geometry of the rock joint is a governing factor for joint mechanical and hydraulic behaviour. A new method for evaluating the aperture distribution, based on measurement of joint surfaces and three dimensional characteristics of each surface, is developed. This method allows one to determine and visualize the aperture distribution under different normal stresses and shear displacements, which is difficult to observe experimentally. A new laser scanner system is designed and developed for joint surface measurements. Special attention is paid to both surfaces' data gained by measurements and processing, such as x-y coordinate table modification, data referencing, and matching between upper and lower surfaces. The surfaces of an artificial joint in granite are measured, processed, analyzed and three dimensional approaches are carried out for surface characterization. Parameters such as ''asperity's heights'', ''slope angles'', and ''aspects'' distribution at micro scale, local concentration of elements and their spatial localization at local scale are determined by Geographic Information System (GIS). These parameters are used for joint surfaces matching and its real behavior quantitative analysis. The upper surface is brought down to make contact with the lower surface and the distance between the two surfaces is evaluated from the joint mean experimental aperture, which is obtained from normal and shear tests. Changes of aperture distribution at different normal stresses and various shear displacements are visualized and interpreted. Increasing normal load causes negative changes in aperture frequency distribution which indicates high joint matching. However, increasing shear displacement causes a rapid increase in the aperture and positive changes in the aperture frequency distribution, which could be due to un-matching, surface anisotropy and spatial localization of contact points with proceeding shear.

Keywords: Rock joint, laser scanner, joint surfaces morphology, GIS, aperture distribution, aperture visualization, joint shear.

1. Introduction

Design and construction of deep underground structures utilize rock mass characteristics such as high-rigidity, sealing, durability and isolation. More severe design conditions and more accurate properties of rock mass are needed in these cases from safety, economical and environmental points of view. Most of the latest proposed underground developments employ sealing and isolation properties of rock mass. It is therefore important to examine the permeability of rock mass where the underground structures are to be constructed, in order to confirm its capacity to isolate. The first step in understanding the rock mass conductivity is the analysis of single rock joint conductivity. The hydraulic conductivity and mechanical behaviour of the joint depend on its surface morphology as well as aperture distribution.

Several techniques have been used for aperture measurement which could be categorized in the two main groups of direct and indirect methods. Direct methods include injection, X-ray Computer Tomography (CT), and Nuclear Magnetic Resonance Imaging (NMRI). Indirect methods use joint surfaces data obtained from touch-type mechanical profile-meter, laser scanner or photo-grammetry, to calculate the joint aperture distribution. Although the proposed aperture measurement methods have improved the understanding of aperture determination, a precise method to evaluate the aperture distribution under different normal and shear loading conditions is not yet available.

Direct aperture measurement methods (Gale, 1987; Gale et al., 1990; Hakami, 1992, 1995) use resin injection techniques. Pyrak-Nolte et al. (1987) used wood metal injection under normal stress to evaluate joint aperture. Gentier et al. (1989) and Hakami (1992) made transparent replicas of void spaces of joints and determined the aperture through image analysis of sections. Making aperture and surface replicas is known as a destructive method where the use of the same specimen for aperture determination and experimental test is not possible. In addition, these methods have low accuracy because the viscosity of the injected material prevents filling of small voids. Furthermore, thick cutting intervals provide only limited data of aperture. Kumar et al. (1997) and Dijk and Berkowitz (1999) used the NMRI to measure the aperture distribution. Johns et al. (1993), Keller (1998), Ohtani et al. (2000) and Stephanie et al. (2001) used the X-ray CT technique for aperture measurement. The X-ray CT and NMRI methods have low spatial resolution, high cost and difficulties with calibration, measurement and analysis.

By indirect aperture measurement methods, Brown and Scholtz (1985) and Gentier (1986) measured joint surfaces topography by the mechanical touch-type profile-meter. For each surface, the surface height and location is continuously recorded. The upper surface is brought to the opposing surface and the aperture is computed by knowing the distance between the joint surfaces. Measuring topography, by the mechanical touch-type profile-meter, has low accuracy due to wide measurement intervals and difficulty in measuring sharp points. This method could also damage the surface. Furthermore, there is difficulty in referencing and matching the two surfaces.

Esaki et al. (1995) and Iwano and Einstein (1995) introduced the laser scanner instead of the mechanical profile-meter to overcome these difficulties. They succeeded in measuring surfaces within very small intervals about 0.5–1.0 mm without specimen

damage; also they used special marked points to reference the upper surface to the lower one. Later, Lee and Cho (2002) also used similar methods for aperture determination. In particular, Hans and Boulon (2003) used the laser scanner for joint surfaces measurement at each defined shear displacement during the test and calculated the aperture using the surface data. All aperture measurement techniques have advantages and limitations that must be chosen depending on the study to be carried out.

Joint aperture determination using asperity data is completely dependent upon joint surface characteristics and comprehensive surface roughness characterization, which can lead to correct aperture determination. Roughness can be explained as local departures from planarity and many researchers so far have presented two dimensional characteristics of surface roughness using profiles. However, surface irregularity, heterogeneity and anisotropy cannot be depicted in two dimensions. Statistical (Tse and Cruden, 1979), geo-statistical (Gentier et al., 2000) and fractal (Kulatilake et al., 1995; Xie et al., 1997; Lanaro, 2000; Fardin et al., 2001) analyses are also used to characterize surface morphology. However, one major problem is the inability of reproducibility, where surfaces with similar statistical or fractal values show different spatial distributions.

Even though these approaches are useful to improve our understanding of roughness, they are not sufficient for three dimensional roughness characterization. Surface roughness is spatially localized and it is necessary to characterize the surface using three dimensional characteristics. Several attempts have been made to present three dimensional characteristics of a surface. Gentier et al. (1997), Lanaro (2000), Belem et al. (2000), Grasselli and Egger (2000, 2003) and Sharifzadeh et al. (2004a) are among the few researchers who have taken into consideration the three dimensional characteristics of joint surfaces such as surface aspect and anisotropy to explain the mechanical behaviour of a joint.

Research shows that aperture is dependent upon stress history, normal displacement, shear displacement and scale of study. Even though aperture measurement and its distribution analysis have been conducted by previous researchers, yet the above problems remain unsolved. Hydro-mechanical tests provide the only result for whole test specimen. However, the micro-mechanism of aperture and contact distribution, asperity deformation and flow test process inside the joint is not clear. This study is intended to determine, visualize and interpret aperture distribution under different normal stress history and various shear displacements in three dimensions.

2. Procedure for Determining the Aperture Distribution

The procedure to obtain a precise aperture distribution using joint surfaces data is illustrated in Fig. 1. The application of an originally designed and developed high resolution laser scanner is justified for joint surfaces asperity height measurement. Errors in surface data originated from laser measurement system and specimen installation on x-y positioning table are rectified by this method. Upper and lower surfaces are characterized and their comparison is used to confirm matching of the joint surfaces.

Moreover, a normal loading test to determine the initial aperture at different normal stresses and a direct shear test to determine the aperture changes during shear are performed. Finally, the joint surfaces and aperture data are integrated in GIS to

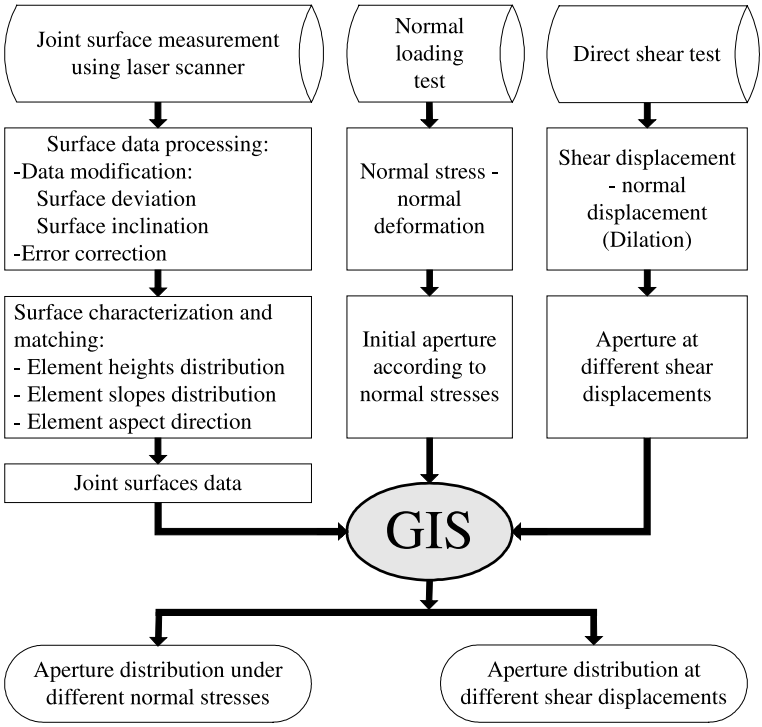

Fig. 1. Procedure for determination of aperture distribution

determine the aperture distribution. Aperture distribution is determined and visualized under different stress and displacement conditions. Variations of aperture distribution during normal and shear loading are quantified by using both aperture distribution maps and aperture frequency distribution.

3. Joint Surface Measurement and Characterization

The rock joint surface roughness plays a major role in the joint mechanical and hydraulic behaviour. Therefore, it is clear that a precise measurement of a rough surface topography is a key to understanding the joint mechanical and hydraulic behaviour in particular during shear. It is obvious that the contribution of roughness in hydro-mechanical models strongly depends on the method of surface measurement and quantification.

For more accurate measurements of joint surfaces morphology, a new device using laser beam was designed and developed (Fig. 2a, b). Surface data were measured on a virtual grid mesh with square elements 0.2 mm in size (Fig. 2c). The measurement area was set wider than the specimen surface area. Then GIS was used to extract real surface data, to check several possible errors, and to correct them. Finally, both surfaces' three dimensional characteristics were determined again by using GIS.

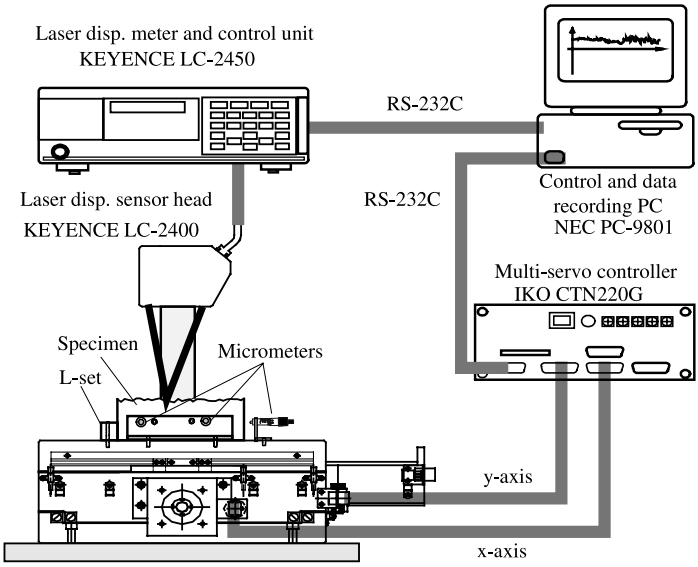

a) Schematic view of three dimensional laser scanner system

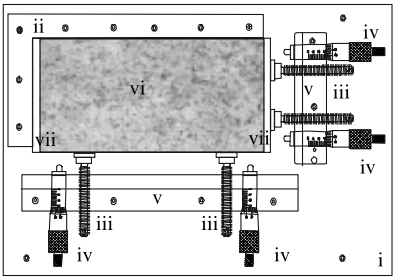

i) Modification tools base plate, ii) L-set, iii) Fixing screw pins, iv) Micrometers, v) L-shape holders, vi) Specimen, vii) Steel plates

b) Plan view of improved laser scanner table

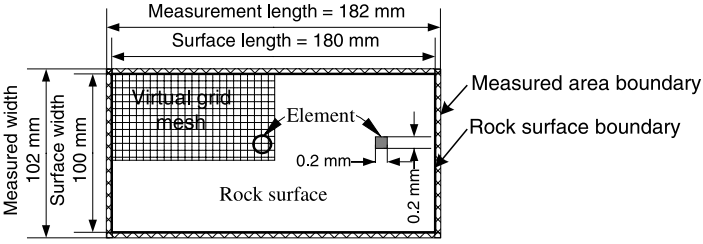

c) Schematic view of surface measurement on virtual grid element

Fig. 2. Schematic view of designed laser scanner and modified table for joint surfaces measurement (not to scale)

3.1 Laser Scanning Apparatus and Measurement Procedures

To obtain precise measurements of the asperity height, a new device using laser beam was designed and calibrated (Fig. 2a). The new device consists of: 1) laser displacement sensor head, with resolution of 0.5 μm, spot size of 45×20 μm and measurement height range of ± 8 mm, 2) x-y positioning table, with stroke area of 250×150 mm, having positioning accuracy of ± 15 μm and repositioning accuracy of ± 3 μm, 3) multi-servo controller of x-y table, 4) laser displacement sensor head controller, and 5) data recording and control devices.

In this system, the distance between the rough surface and the laser gauge is measured as z-elevation by the measuring head. The zero reference position and the intervals of measurement in x- and y-directions are controlled by the positioning table controller. The asperity data are first measured in the x-direction, then the table moves in y-direction with defined intervals. The process is repeated until the whole surface measurement is completed. This system has the capability of setting area and intervals of measurement in arbitrary values.

One of the most important difficulties of this technique (surface topography) – especially for joint aperture determination – is its high sensitivity to referencing the specimen (the upper and lower halves with respect to each other) and matching the joint surfaces based on their measured asperity height. To overcome this problem, both the experimental surface measurement method and the surface data analysis method have been improved to achieve matching between the two surfaces (Sharifzadeh et al., 2004b). As shown in Fig. 2b, a positioning table is equipped by the so called ''Setting Block'' with micrometers and pins to fix the specimen on the table, in order to prevent possible specimen displacements during measurement. Four sides of the specimen are kept tight; the Setting Block is held at the two sides, as the other two sides are kept by placing two pins at each side situated beside the micrometers (Fig. 2b). Micrometers perform a double duty before and after surface measurement. The specimen position is measured by two micrometers at each side in order to compare whether the repositioning of the specimen is achieved or not. The results of the micrometer measurements are used to set the other half of the specimen at the same position as the previous measured half.

In this study, a granite block of $180 \times 100 \times 80$ mm (length $\times$ width $\times$ height) was used. An artificial rock joint was chosen in order to increase reproducibility. This artificial joint was created at mid-height of the specimen. An apparatus was built for creating each joint as described in detail by Esaki et al. (1998). The apparatus consists of a couple of horizontal jacks and a normal loading jack. The horizontal jacks are attached to the long side of the specimen for creating the joint by splitting it with a couple of steel wedges, in order to control the aperture of the joint. For stability in creating the joint, a constant horizontal load for splitting is applied through a pair of wedges, after applying a prescribed normal load on the specimen. Then, the normal load is gradually reduced during fracturing while the horizontal load is kept constant. Thus, the joint is made stable under controlled conditions and can be used for surface measurements.

The procedure for surface measurements consists of: i) placing the specimen upper or lower surfaces on the x-y positioning table, ii) tightening the long side and then the

short side pins and measuring the long side and short side micrometers, iii) setting the coordinate of the starting point for measurement, iv) inputting the different parameters into a PC (starting point, number of lines and intervals in x- and y-directions), and finally v) running the code. The x-y table coordinates and the corresponding z values measured by the laser scanner are stored automatically.

3.2 Laser Scanner Calibration

Several parameters are important for accurate measurements, such as: i) temperature, ii) average measurement frequency, iii) table stopping time for laser radiation – reflection, iv) installation of laser displacement meter, and v) x-y positioning table movement speed. These parameters can be fixed based on the rock conditions and measurements. Efforts were made to isolate the changes of temperature and light intensity during day and night. However, errors due to small changes are often unavoidable. The calibration of the specimen setting and of the x-y positioning table speed for laser measurement is explained below.

A 40×20 mm area in the center of the specimen was selected and several measurements in the same condition were repeated with respect to the long side and the short side setting and with different table speeds. For setting up the specimen on the table and giving the priority of tightening the pins at the long side or short side, five measurements for each setting were repeated and the standard deviation of the settings was determined. The standard deviation with respect to the long side was 3.4×10^{-2} μm and along the short side 3×10^{-2} μm. Since the long side standard deviation is less than that of the short side, the long side setting is to be made prior to short side setting. In other words, at first it is better to tight the long side pins and then to tight the short side ones.

The effects of the table speed, stopping time for each laser measurement and loop number on the accuracy of laser scanner measurement results were checked with different speeds and standard deviations of measurements. It is noteworthy that the loop number is representative of the table speed and that a low loop number indicates slow movement or long stopping time of the table and viceversa. The results obtained show the same standard deviation up to 300 loops and after that a gradual increase is observed. Therefore, 300 loops is chosen for measuring (Fig. 3). This system is used for precise measurements of the joint surfaces mesh element height.

3.3 Joint Surfaces Data Processing

GIS technology along with specifically developed computer programs was implemented to measure the asperity heights, to process the data and evaluate possible deviations and inclination corrections in order to obtain spatial positioning and matching of the joint surfaces. A virtual mesh having a square element size of 0.2 mm spread on each surface and each element height was measured by the laser scanner (Fig. 2c). It should be noted that, based on the surface asperity conditions, each element could be an asperity or several elements might form one asperity. In other words, selected measurement intervals or element size are small enough to represent an asperity. Thus,

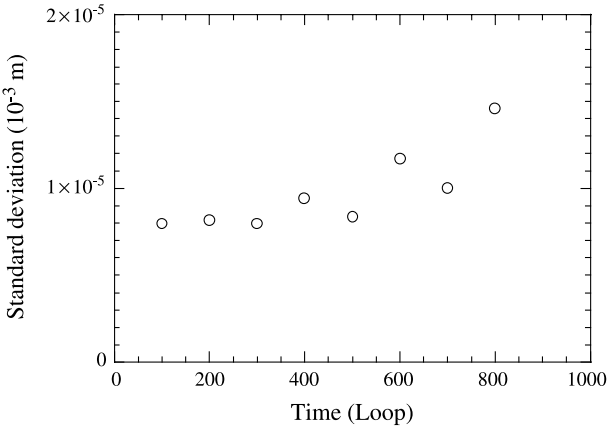

Fig. 3. Accuracy test for table stopping time

in some cases one element could be used as asperity or several elements with each other could form an asperity.

Each half was placed on the laser scanner table and the surface element height was measured with 0.2 mm intervals in x- and y-directions. Measured surface data were checked against possible installation and intrinsic laser measurement errors. Possible errors originated from specimen installation, such as surface deviation from x-y plane and inclination from x-z and y-z planes, were checked as shown in Fig. 4. The procedure for surface deviation check is illustrated in Fig. 5. To avoid loosing surface data, the measurement areas were set 1 mm wider (182 × 102) compared to the original size. A total of 464,100 elevation data were obtained on each surface with their x- and y-coordinates.

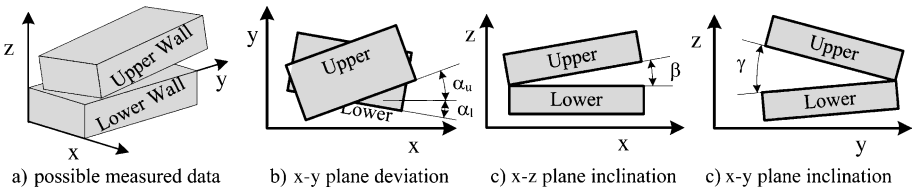

Fig. 4. Errors originated from specimen installation on laser scanner table

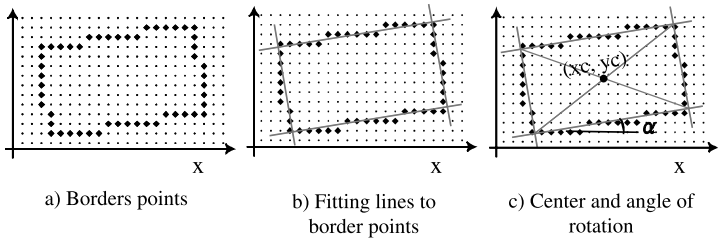

Fig. 5. Selection of real surface data from measured data

The Geographic Information System (GIS) is used to visualize and define the real surface mesh element height data from extra error point data. Surface data are classified in different height classes. GIS-selection tools are used to find the border of the real rock joint surface from adjacent error points (Fig. 5a). Real surface border lines are determined by linear fitting of selected border points (Fig. 5b). Border lines equations are used to calculate the joint center (x_c, y_c) and the angle of surface long side line from x-axis (Fig. 5c).

By comparing the long side border lines, equations of both surfaces deviated from the x-y plane and differences in border lines deviation are calculated. The deviated surface data are rotated back to fit each other. In this study, the difference between the upper and the lower surface border line angle is $\alpha = 0.145^\circ$, which is corrected by rotating the upper surface data with respect to the center of the specimen.

In order to check the x-z and y-z plane inclinations (Fig. 4c), the surface equation for each surface is calculated using the element height data. Equations for both the lower and upper surface are compared to each other to check the parallelism and inclination of surfaces as shown in Fig. 4c. In this study, the upper and lower surfaces equations are determined as follows:

$$\begin{cases} \text{Lower Surface equation:} \;\; z = -0.00005x + 0.00017y - 1.378 \\ \text{Upper Surface equation:} \;\; z = -0.00005x + 0.00022y + 0.895 \end{cases} \quad (1)$$

Equation (1) shows the joint surface equation for the sample under study. Comparison of the lower and upper surface equations shows close similarity between the two surfaces, hence the joint surfaces are assumed to be parallel. Finally, the data of joint surfaces with a total of 449,599 heights and over 180×99.8 mm area are extracted.

Intrinsic errors from laser measurement are due to the differences of laser light reflection from dark and bright minerals on surfaces. Errors occurred from laser measurement noise give an out of scale value (± 99.99 in mm) and an abnormal z-value (larger than five times the data standard deviation) in some points. In this case there were 20 points (12 points in the lower and 8 points in the upper surface) with z-value of ± 99.99 in mm and 83 points (51 points in the lower and 32 points in the upper surface) with z-value greater than five times the standard deviation.

The error points in both the upper and lower surfaces are corrected by using the average of neighboring points elevations. Since the joint upper surface is turned back to set on the laser scanner table, after obtaining the real surface, the upper surface data are numerically overturned to represent its natural condition in the joint. The results in terms of the modified surface mesh element heights of both the upper and lower surfaces data are saved as ASCII grid and xyz format, to be used for joint aperture assessment.

3.4 Joint Surface Characterization

To evaluate the surface data and modification methods discussed in the previous section and to verify the capability of referencing the joint surfaces, the upper and lower surfaces characteristics are determined and compared with each other, in order to check whether they match or do not. Most researchers so far have focused on two-dimensional simulation of surface roughness, although the actual morphology is

three-dimensional. Basically, the surface roughness is most often described by some linear parameters calculated in individual profiles which are obtained along one-directional parallel lines (Belem et al., 2000). The parameters describing the entire surface of the fracture can be obtained by calculating the average of parameters of all profiles (Barton, 1982). Hence, a three dimensional problem is solved by a two dimensional approach. However, real geometry should be quantified by three dimensional characterization of the surfaces. Surface asperities have different characteristics: they are not evenly distributed and their distribution depends on spatial position of the surfaces.

In this study, efforts have been made to give three-dimensional interpretations of joint surface roughness and aperture distribution, based on the height of local roughness elements using GIS and statistical parameters. The data of both the upper and lower surfaces mesh elements are converted to ASCII grid as GIS ''raster'' data. Each 0.2×0.2 mm area is measured as one element or point data in mesh on surfaces mesh, and collection of elements form asperities on joint surfaces. Consequently, each surface is defined as a collection of asperities with different heights, slope angles, aspects and positions.

Using GIS three dimensional analysis tools, these characteristics can be analyzed. Each surface is studied with three scales consisting of: i) element or micro-scale, ii) local area scale (or a few square centimeters), and iii) laboratory scale. Micro-scale characteristics are: elements heights, slope angles and aspects determined accurately by using GIS (Fig. 6). Elements concentrations on local area on joint surfaces are presented as local scale characterization.

The first property to consider is the element height. To obtain the height of each element, mean surface data are calculated as base level and elements height is measured with respect to the mean surface. Thus, the element height represents the height from the surface average height. Since the upper and lower surfaces are similar, their mean data is almost similar. Element heights form asperities, joint roughness, and pattern of asperities distribution on the surfaces through which they govern both the mechanical and hydraulic behaviors. Figures 6a, d show the asperity's heights distribution maps and frequency distribution histograms with statistical calculation results. The lower and upper surfaces asperity distribution maps (Fig. 6a, b) and their histograms (Fig. 6c, d) show the normal distribution with mean height from standard line, and standard deviation of 0.7448 and 0.7550 mm, respectively.

The micro and local scale surface comparison shows that a normal distribution is found in micro scale as depicted in Fig. 6c, d and a spatially localized distribution is observed in local scale (Fig. 7a, b) which indicates irregularity of asperities distribution. i.e. although normal distribution of elements heights for whole surface is shown in Fig. 6c, d – and it is expected as a regular asperities distribution – (Fig. 7a, b) irregular changes of asperities are present in the profiles (spatial localization).

The surface mesh element plane angularity, which is the element plane inclination angle with respect to the horizontal plane, will be referred in the following as element ''slope angle''. Slope angle is a direct measure of joint surfaces matching and dilation during a shear process. Figures 6e, f show the slope angle frequency distribution histograms. Both histograms exhibit a log-normal distribution, having

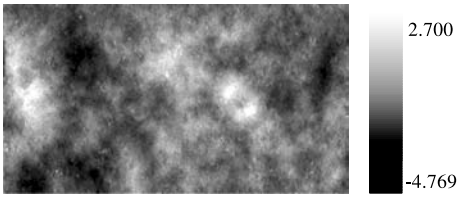

(a) Distribution of lower asperities height

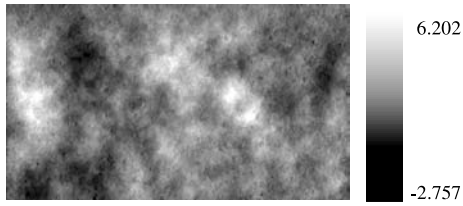

(b) Distribution of upper asperities height

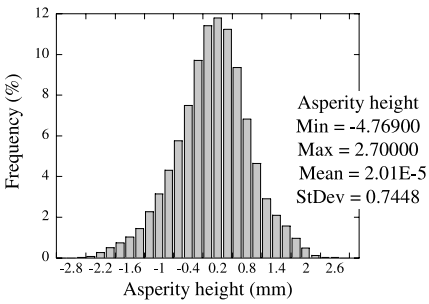

(c) Histogram of lower surface asperities height

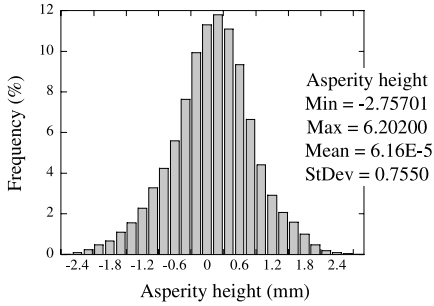

(d) Histogram of upper surface asperities height

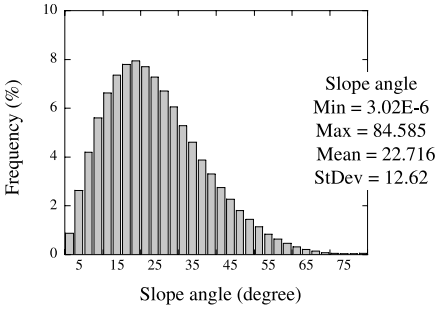

(e) Histogram of lower surface slope angle

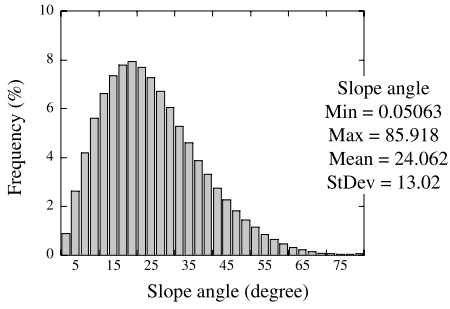

(f) Histogram of upper surface slope angle

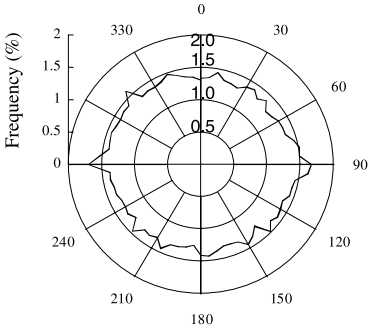

(g) Polar plot of lower surface aspect

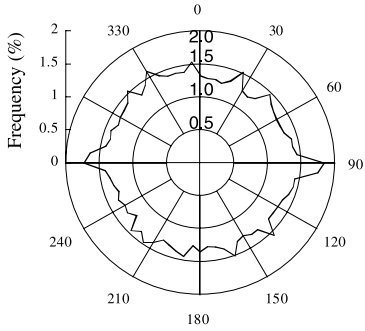

(h) Polar plot of upper surface aspect

Fig. 6. Joint lower and upper surfaces asperitys heights, slope angle, and aspect distribution

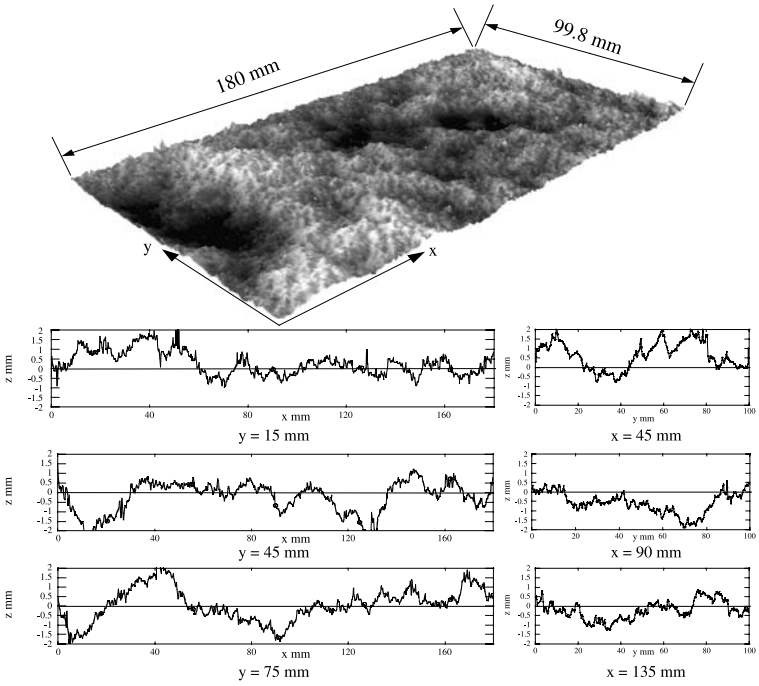

a) Three dimensional view and profiles in x- and y-direction on upper surface

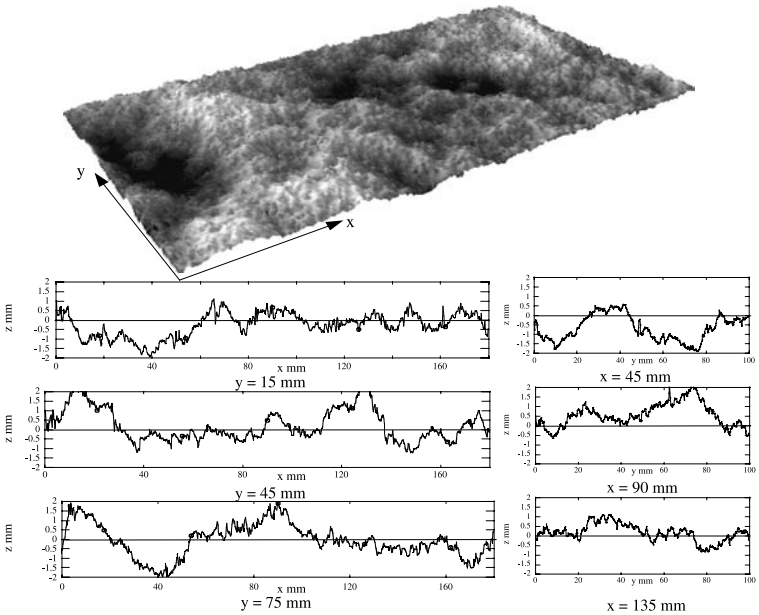

b) Three dimensional view and profiles in x- and y-direction on lower surface

Fig. 7. Upper and lower surfaces three dimensional view along with profiles in x- and y-direction to show surface roughness irregularity and elements concentration on local areas over the joint surfaces

mean slope angles of 22.7 and 24.1°, and standard deviation of 12.6 and 13.0°, respectively.

The surface asperity plane orientation, referred to as ''aspect'' hereafter, is one of the most important characteristics affecting the joint shear behavior. ''Aspect'' is the down slope direction of an element with respect to its neighbor elements and could identify the orientation or direction of slope. ''Aspect'' can be defined as the angle between normal vectors on each triangle from north (shear) direction, which is a projection of plane orientation with respect to shear direction (Grasselli and Egger, 2003). Figures 6g, h show a polar plot of the aspect direction that indicates equal distribution of aspect over joint surfaces. Thus, equal dilation is likely to occur in all the shear directions.

Joint upper and lower surface characteristics are compared to each other to evaluate the capability of the surface morphology measurement and data modification method. Comparison between pairs of upper and lower surface asperity heights, slope angles and aspects direction distribution, as shown in Fig. 6c–h, indicates close similarity between two surfaces which means high matching of joint surfaces. Thus, it could be concluded that the applied data measurement technique (surface topography) is successful to overcome referencing difficulties encountered in former studies and matching between joint surfaces is achieved by using the topography method.

From all of the above mentioned parameters, a three dimensional interpretation of joint surfaces is presented. This analysis can illustrate the aperture distribution during the shear process. Each surface can be defined as a collection of asperities with different heights, slopes, aspects and statistical values. The surface contains a collection of elevated and depressed elements having their own statistical quantities (Fig. 7), which are different from each other. The difference between concentration parameters and their spatial distribution verifies surface irregularity as illustrated in Fig. 7. On the other hand, changes of asperity height trace in line will give two dimensional profiles, which show roughness, waviness and undulation. However, in case of three dimensional characterization, we assumed a spatial distribution of asperities concentration with different characteristics. Therefore, the joint surface behavior not only depends on micro scale characterization, but also on local scale characterization of asperity concentrations, which is spatially distributed unevenly on the surfaces. Therefore, it plays a major role on the shape of joint surface and governs the joint aperture during shear displacement.

4. Initial Mechanical Aperture Under Normal and Shear Loading

To establish the aperture, joint surfaces should be closed to each other. To bring the two surfaces together, the distance between them should be determined. In this study, the distance is calculated from the initial aperture and the dilation data which are obtained from experiments. These apertures are compared with the mean aperture during aperture distribution calculation using the joint asperity height method. Therefore, the distance between two surfaces is a very important parameter in joint aperture distribution determination and must be calculated precisely. In this study a great attention was paid to a precise determination of aperture under normal loading and shear displacements.

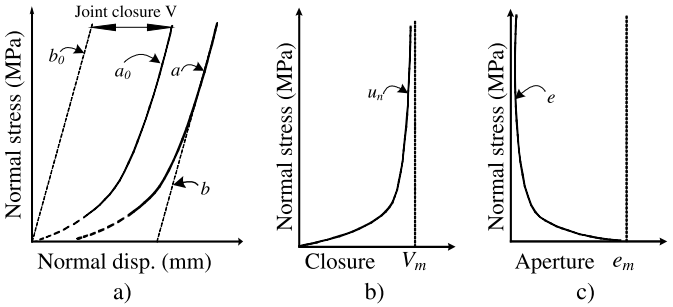

Fig. 8. Procedure for joint initial aperture determination from normal loading test

The initial aperture under different normal stresses is determined. To do this, a normal loading test is carried out on the joint. Normal displacements are measured by four transducers at the four edges of the specimen upper box. Loading of 10 MPa and unloading of 1 MPa is repeated a few times until a stable curve is obtained (Fig. 8a: curve-a). The normal displacement curve comprises the deformation of the joint itself, of the intact part of the rock specimen, and of the shear box.

There are no normal displacement data at low normal stress (dashed line in curve-a in Fig. 8a.) because of the weight of the upper shear box; thus the intersection with the horizontal axis is unknown. To calculate the intercept of curve-a, the normal stress is taken to be 3 MPa and a hyperbolic function is fitted to the data. Therefore, the interception on the horizontal axis is determined and curve-a shifted to the origin (Fig. 8a: curve-a_0). The normal stress is then increased and the normal stiffness remains almost constant and represents the normal stiffness of the intact rock and of the shear apparatus.

Intact rock and apparatus stiffness is calculated from the constant part of curve-a. To do this, the data for a stress value larger than 8 MPa are selected and fitted by a line (Fig. 8a: curve-b) and similarly curve-b is shifted to the origin (Fig. 8a: curve-b_0). After translating curve-a and curve-b to the origin, the normal deformation curve of the rock joint is obtained (Fig. 8b). The closure is approximated by a hyperbolic function as given by Bandis et al. (1983) as follows:

$$\sigma_n = \frac{u_n}{a - bu_n}. \tag{2}$$

Therefore the maximum closure V_m is obtained:

$$V_m = \lim_{\sigma_n \to \infty} u_n = \frac{a}{b}, \tag{3}$$

where σ_n is the normal stress, u_n is the normal deformation, V_m is the joint maximum closure, a, b are sample coefficients.

Initial aperture is calculated by taking the difference of normal deformation from the maximum closure. The joint aperture in relation to the normal stress is obtained as follows (Fig. 8c):

$$e_m = V_m - u_n = \frac{V_m}{1 + b\sigma_n}, \tag{4}$$

where e_m is the initial mechanical aperture or distance between the two surfaces at rest (in mm) and σ_n is the normal stress. For this study, Eq. (4) is written as follows (Fig. 9):

$$e_m = \frac{0.099}{1 + 1.14\sigma_n}. \tag{5}$$

The initial aperture varies from 0.0607 mm at 1 MPa to 0.0087 mm at 10 MPa. Thus, with increasing normal stress up to 4 MPa, aperture decreases rapidly, then to follow a gradual decrease up to 10 MPa. This trend indicates that with increasing deformation and contact area, it becomes more difficult to obtain deformation.

The change of aperture at different shear displacements was obtained from joint dilation during a direct shear test, which was performed on artificial granite joint under 3 MPa normal stress (Fig. 10a). Moreover, during the shear process the upper

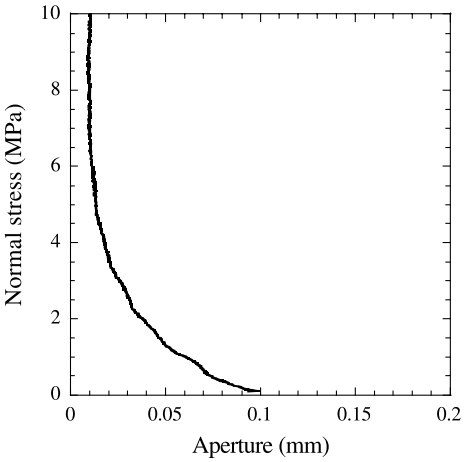

Fig. 9. Joint initial aperture under different normal stresses

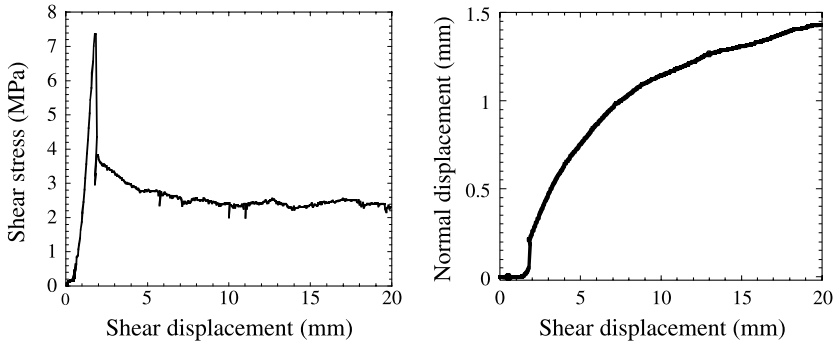

Fig. 10. Shear test results under 3 MPa normal stress, showing the changes of shear stress and normal displacement (dilation) versus shear displacement

and lower surfaces are kept parallel by adjusting the normal load on the front and rear normal jacks.

Prior to shearing, it is noteworthy that a uniaxial compression test is also carried out on a granite intact specimen. The uniaxial compressive strength of the rock material is 165 MPa which identifies a very hard rock. Normal stress during shearing is very low compared to the rock strength. Thus, it is assumed that under this condition, gouge material will not be produced and asperities will behave as rigid material. No asperity damage is considered in this research.

Changes of shear stress and normal displacement with respect to shear displacement are shown in Fig. 10a, b. The normal displacement before shear (at zero shear displacement) is obtained from joint initial aperture curve as in Sect. 4. Shear displacement proceeded up to 20 mm, and the changes of normal displacement during shearing are shown in Fig. 10b. Small contractions are observed up to 1.5 mm of shear displacement because of locking of the asperities of the upper and lower surfaces. This is followed by a sudden increase in normal displacement (dilation), as the shear stress increases simultaneously up to peak. After that, the shear stress rapidly decreases to the residual stress value and becomes almost constant (Fig. 10a). The changes of normal displacement during shearing were used to determine the aperture at different shear displacements.

As a result, the distance between the joint surfaces for aperture distribution analysis is determined from initial aperture according to normal stresses and changes of aperture at different shear displacement. These data will be used as a part of input data for aperture distribution analysis.

5. Aperture Distribution at Normal and Shear Loading

To obtain the aperture distribution using surface asperity heights data, the two halves of the specimen are brought into proximity with each other. For this purpose, the lower surface is kept fixed and the upper surface is brought down to form the aperture. By assuming that two surfaces are coincident (point by point), the aperture can be defined as the distance or gap between two corresponding elements on both joint surfaces mesh.

The joint aperture distribution is determined using the newly defined surface characteristics, integrated in GIS (Sharifzadeh, 2005). This can be performed by importing the upper and lower surfaces x-, y- and z-data in GIS. By using the GIS tools, the information on two surfaces can be calculated and new data tables are created. Each data table consists of four columns: the x-, y-coordinate and z-elevation of the upper and lower surfaces simplified as the same x-y having two z-elevation values.

With the same x-y-grid and different z-elevations new data creation becomes possible. New columns showing the piecewise aperture are created and the mean value of each column is calculated and compared with the aperture obtained from experiment (aperture from previous section). When the mean column value becomes equal to the initial aperture, calculations are stopped and the results are the aperture values for the specific case.

During the shear process (as in a real shear testing machine) the lower surface grid data are moved to the left in steps of given size. This procedure is repeated until the completion of all the columns for different normal stresses and shear displacement

conditions. The aperture distribution can be visualized in GIS using these data and statistical parameters. Elements with negative and null values represent elements in contact or compression and are assumed as contact points. Elements with positive values represent the aperture. The mean aperture and the contact ratio are calculated and the data table is used to show the aperture frequency distribution histograms.

5.1 Aperture Distribution at Different Normal Stress

The aperture distribution varies with the normal stress and can be calculated and visualized using the above mentioned method. Figure 11 shows the aperture distribution map (left), its frequency distribution, the mean aperture and contact ratio at 1, 3, 5 and 10 MPa normal stress. In Fig. 11a, d, the contact ratio increases from 84.8 to 98.4%, while the mean aperture decreases from 43.97 to 7.29 μm for the normal stress increasing from 1 to 10 MPa, which shows a high degree of matching between the two surfaces and proves the surface measurement and processing technique to be effective as a correct aperture determination method.

The frequency distribution histogram of the aperture is presented in Fig. 11 (right). Both surfaces asperities heights follow the Gaussian distribution. However, the aperture frequency distribution under normal load is found to be similar to the Poisson or Log-normal distribution. Increasing the normal stress causes a drop in aperture, and an increase in the contact ratio, resulting in a negative change (shifting to the left) in aperture frequency distribution, and indicating that the whole surfaces come into close contact and therefore high matching between two surfaces is found. At high normal stress, the contact ratio is almost 100% and the joint is completely closed which indicates that the joint behaves as intact rock. However, a small value of aperture is still remaining.

5.2 Aperture Distribution at Different Shear Displacements

Changes of aperture distribution during shear are illustrated by a three dimensional surface characterization based on the results of shear experiments. Figure 11b shows the aperture distribution map (left) and the frequency distribution (right) before shearing and Fig. 12a–h show the change of aperture distribution map (left) and aperture frequency distribution (right) during different shear displacements. In this study the effect of the gauge material is neglected.

Comparison of the aperture maps with aperture frequency distribution before shearing shows that the contact elements are distributed equally because of a good matching between two surfaces (Fig. 11b). With increasing shear, at initial sliding some asperities leave contact, thus the contact ratio decreases and the mean aperture increases significantly, but the aperture and contact pattern still shows an even distribution (Fig. 12a, b).

At critical point near peak shear, where the shear stress is in equilibrium with the strength of the asperities in contact (Fig. 9a), an increment of shear causes simultaneous shearing of all the asperities in contact. Consequently, a sudden change in aperture distribution occurs due to un-matching between the two surfaces. At this stage,

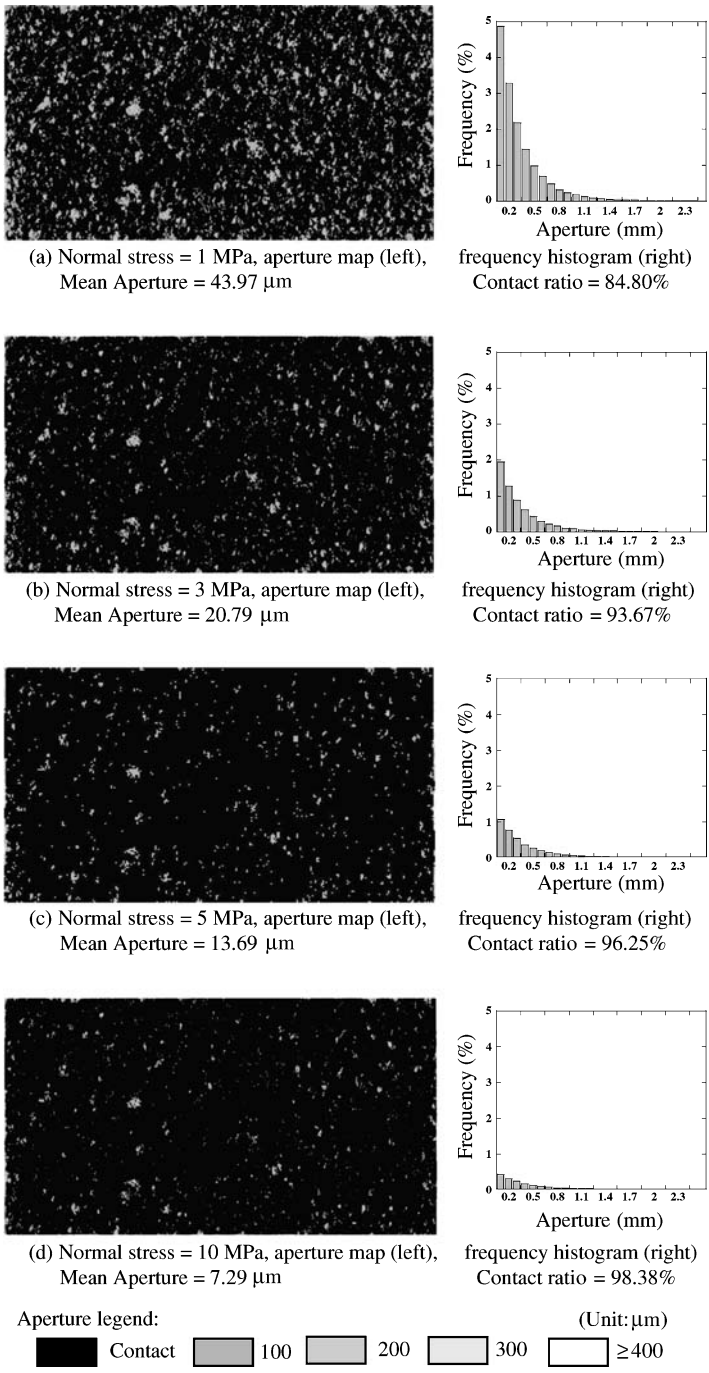

Fig. 11. Aperture distribution map (left) and frequency distribution (histogram-right) with mean aperture and percent of contact ratio under different normal stresses

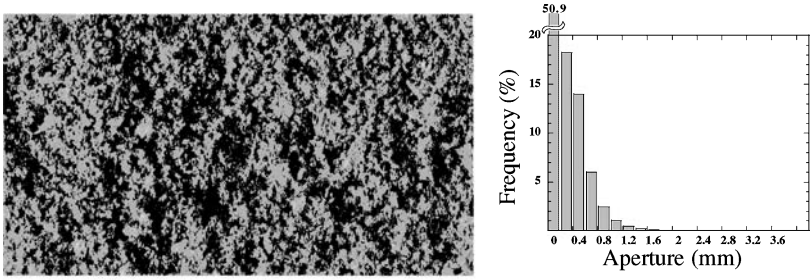

(a) Shear displacement 1 mm, aperture map (left), frequency histogram (right)
Mean Aperture = 131.19 μm Contact ratio = 50.8%

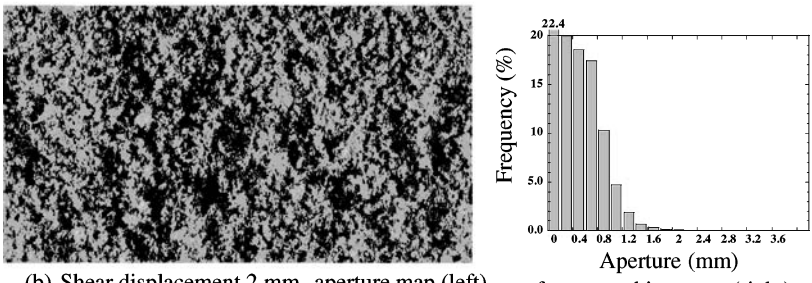

(b) Shear displacement 2 mm, aperture map (left), frequency histogram (right)
Mean Aperture = 325.13 μm Contact ratio = 22.4%

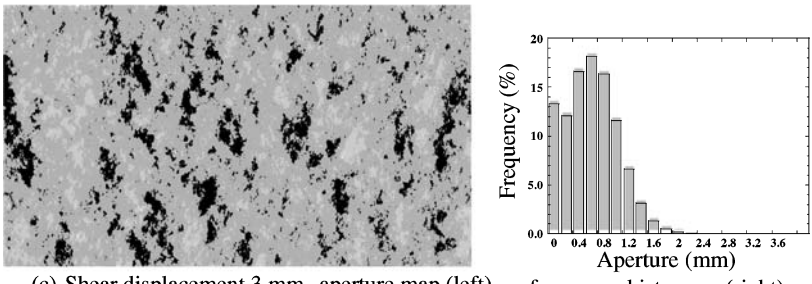

(c) Shear displacement 3 mm, aperture map (left), frequency histogram (right)
Mean Aperture = 520.76 μm Contact ratio = 13.3%

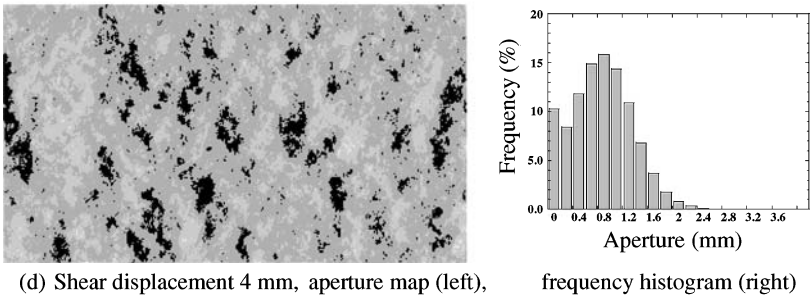

(d) Shear displacement 4 mm, aperture map (left), frequency histogram (right)
Mean Aperture = 677.78 μm Contact ratio = 10.3%

Fig. 12. Aperture distribution map (left) and aperture frequency distribution (histogram-right) with mean aperture and percent of contact ratio at different shear displacements (under 3 MPa of normal stress)

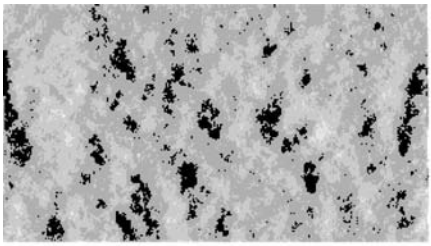
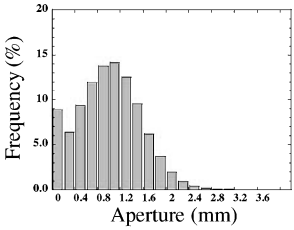

(e) Shear displacement 5 mm, aperture map (left), frequency histogram (right)
Mean Aperture = 807.48 μm Contact ratio = 8.9%

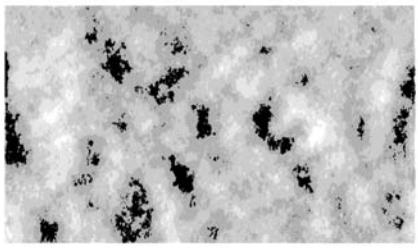
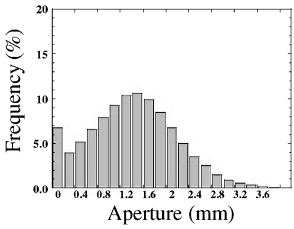

(f) Shear displacement 10 mm, aperture map (left), frequency histogram (right)
Mean Aperture = 1213.21 μm Contact ratio = 6.7%

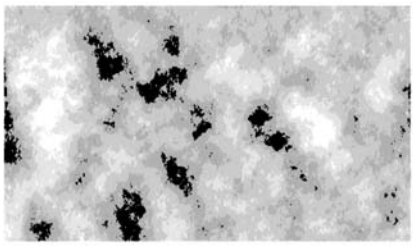
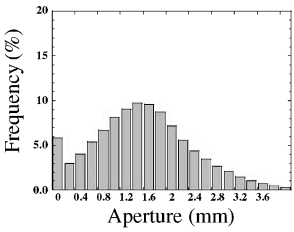

(g) Shear displacement 15 mm, aperture map (left), frequency histogram (right)
Mean Aperture = 1402.64 μm Contact ratio = 5.9%

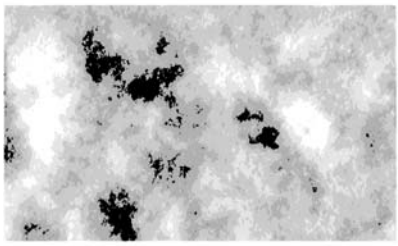
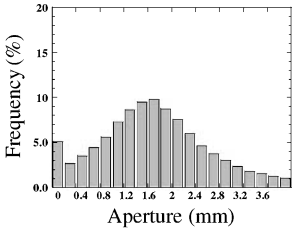

(h) Shear displacement 20 mm, aperture map (left), frequency histogram (right)
Mean Aperture = 1539.96 μm Contact ratio = 5.1%

Aperture legend: (Unit: μm)

Fig. 12 (*continued*)

micro scale asperities loose contact and localized areas remain in contact as shown in Fig. 12c–e. Aperture and contact are spatially localized; as a result, the ratio of the contact area decreases and aperture increases rapidly.

Finally, with increasing shear displacement, dilation becomes controlled by the next asperities in shear and consequently un-matching increases between the surfaces. Distribution of contact area is spatially localized on certain asperities and the mean aperture and contact ratio show slight change (Fig. 12h). Aperture frequency distribution is presented in Fig. 12 (right). The contact ratio varies from 93.6% before shear to 5.1% at 20 mm of shear displacement. The aperture values change from 20.79 μm before shear to 1.54 mm (539.96 μm) at 20 mm of shear displacement.

Increasing shear causes an increase in aperture and a decrease in contact ratio. Following aperture frequency histograms show that although at first aperture frequency distribution follows a Poisson distribution, with increasing shear an increase in aperture frequency which can be described with normal distribution curve occurs. The results show that, for shear displacement before peak, the aperture and contact area values are evenly distributed. With increasing shear displacement, particularly in residual region, spatially localized and heterogeneous distribution of aperture is observed due to anisotropy and un-matching of surfaces.

6. Discussion

Aperture is very sensitive to changes of joint surface morphology and applied conditions such as changes of normal and shear load. A newly developed laser scanner is capable to measure joint surface with very small element (grid) size of 0.2×0.2 mm. This element size is small enough to study the surface morphology. Combination of measured data in GIS is found to be a powerful tool to calculate and visualize the surface characteristics and their comparisons. In micro scale, asperity heights, slope and aspects are determined using GIS.

In local scale the ''elements concentration'' concept is presented by aperture distribution maps and used for a three dimensional characterization of the surface. Each surface is described as several elements concentrations with spatial distribution on surfaces and each concentration has its own concentration (statistical) value.

Based on this concept, the surface asperity frequency distribution is shown to follow the Gaussian frequency distribution. However, concentration of elements on local scale shows roughness irregularity and spatial distribution, which cause surface anisotropy and heterogeneity. Surface anisotropy and heterogeneity is the main source of joint complex behaviour and un-matching with small displacement.

Furthermore, the determination of distance between two surfaces from aperture calculated through experiments makes it possible to verify the aperture distribution on joints with the same element size as the surface measurement. Finally, the aperture distribution is determined and visualized under different normal stress values and shear displacements using joint surface data and initial aperture integrating in GIS. Changes of aperture distribution during normal and shear process are interpreted using both aperture distribution maps and aperture frequency distribution.

Aperture distribution during normal loading shows that: i) aperture is evenly distributed, ii) findings at micro-scale aperture (Fig. 11) are verified at macro scale

(Figs. 8 and 9), and iii) aperture decreases with increasing of normal stress and reaches the residual value. Moreover, the aperture distribution during shear shows that: i) before peak shear, aperture is randomly distributed; however, after peak shear, aperture distribution is spatially localized with increasing shear and depends on surface anisotropy, ii) joint surfaces anisotropy and heterogeneity is the main cause of spatial localization of aperture distribution, and iii) contact ratio decreases rapidly and reaches a quite small value for a large shear displacement after peak shear stress.

It is hoped that the analysis of surface and aperture distribution at small scale would enable one to make a local scale study of the hydraulic and mechanical behaviour. Hence, mechanical and hydraulic properties can be specified locally for each element with different characteristics and superposition of them which represent the whole specimen behaviour (Sharifzadeh, 2005).

7. Conclusions

In this study, efforts have been made to establish a new three dimensional joint surface measurement and characterization method, to determine the aperture distribution precisely and visualize it under normal and shear loading. An originally designed and developed laser scanner is capable to measure the surface mesh element height with high resolution in z-elevation and very small intervals with high accuracy in x- and y-directions. An improvement in both asperity heights measurement techniques and processing was obtained for referenced and matched surfaces.

The joint surface processing and analysis in GIS not only show high matching between two surfaces but also make it possible for three dimensional characterization of surfaces. Some important parameters are evaluated such as asperity heights, slope angle, aspects and concentration of asperities on local areas. Although asperity heights frequency distribution for whole surface follows the Gaussian frequency distribution, local concentration of elements distribution shows spatial localization which causes surface irregularity, anisotropy and heterogeneity.

Three dimensional characteristics of the surface are used for a better understanding of the joint real behavior and illustrate aperture and contact distribution changes under shear loading. The two surfaces are overlapped numerically to form the aperture and bring them to contact with each other until a specific distance (aperture obtained from experiment) is achieved. The distance is obtained from initial aperture and normal loading test and also from dilation data at different shear displacements.

Aperture distribution is determined and visualized under given normal stress and shear displacements using GIS calculation and visualization tools with element size of 0.2×0.2 mm. In addition, mean aperture, contact ratio and aperture frequency distribution are determined. Aperture distribution is illustrated by using developed three dimensional surface characteristics.

Increase in normal stress causes slight increase in contact ratio and decrease in aperture size which causes negative changes in aperture frequency distribution, with homogenous aperture distribution. These results indicate that matching of the surfaces increases with increasing normal stress and without any shear displacement.

Increases in shear displacement causes rapid increase in aperture size and decrease in contact ratio, which causes positive changes in aperture frequency distribution,

resulting in a spatial localization and heterogeneous distribution of the aperture. The surfaces anisotropy is the main reason for the heterogeneity in aperture distribution, thus producing un-matching between the surfaces with increasing shear displacement.

References

Bandis, S. C., Lumsden, A. C., Barton, N. R. (1983): Fundamentals of rock joint deformation. Int. J. Rock Mech. Min. Sci. Geomech. Abstr. 20(6), 246–268.

Barton, N. (1982): Modeling rock joint behavior from in situ block tests: Implication for nuclear waste repository design. Technocal report ONWI-308, Colombus, Ohio.

Belem, T., Homand-Etinne, F., Souley, M. (2000): Quantitative parameters for rock joint roughness. Rock Mech. Rock Engng. 33(4), 217–242.

Brown, S. R., Scholtz, C. H. (1985): Broad bandwidth study of the topography of natural rock surfaces. J. Geophys. Res. 90, No. B14, 12,575–12,582

Dijk, P., Berkowitz, B. (1999): Investigation of flow in water saturated rock fractures using nuclear magnetic resonance imaging (NMRI). Water Resour. Res. 35(2), 347–360.

Esaki, T., Ikusada, K., Akikawa, A. (1995): Surface roughness and hydraulic properties of sheared rock. In: Proc., Fractured and jointed rock masses. Balkema, Rotterdam, 393–398.

Esaki, T., Shouji, D., Jiang, Y., Wada, Y., Mitani, Y. (1998): Relationship between mechanical and hydraulic aperture during shear – flow coupling test. In: Proc., 10th Japan Symposium on Rock Mechanics, 91–96.

Fardin, N., Stephenson, O., Jing, L. (2001): The scale dependence of rock joint surface roughness. Int. J. Rock Mech. Sci. Geomech. Abstr. 38, 659–669.

Gale, J. E. (1987): Comparison of coupled fracture deformation and fluid flow models with direct measurements of fracture pore structure and stress-flow properties. In: Proc., 28th U.S. Symposium on Rock Mechanics. Balkema, Rotterdam, 1213–1222.

Gale, J., MacLoad, R., LeMessurier, P. (1990): Site characterization and validation – measurement of flow rate, solute velocities and aperture variation in natural fractures as a function of normal and shear stress, stage 3. Stripa project. Technical report TR 90-11. SKB, Stockholm.

Gentier, S. (1986): Morphologie et compartment hydrome ćanique d'une fracuture naturelle dans un granite sous contrainte normale, PhD thesis, Univesite d'Orleáns, Orleáns, France.

Gentier, S., Billaux, D., van Vliet, L. (1989): Laboratory testing of the voids of a fracture. Int. J. Rock Mech. Rock Engng. 22, 149–157.

Gentier, S., Hopkins, D. L. (1997): Mapping fracture aperture as a function of normal stress using a combination of casting, image analysis and modeling techniques. Int. J. Rock Mech. Min. Sci. Geomech. Abstr. 34, 359.

Gentier, S., Riss, J., Archambault, G., Flamand, R., Hopkins, D. L. (2000): Influence of fracture geometry on sheared behavior. Int. J. Rock Mech. Min. Sci. Geomech. Abstr. 37, 161–174.

Grasselli, G., Egger, P. (2000): 3D surface characterization for the prediction of the shear strength of rough joint. In: Proc., Eurock 2000, Aachen, Germany 281–286.

Grasselli, G., Egger, P. (2003): Constitutive law for rock joints based on 3-D surface parameters. Int. J. Rock Mech. Min. Sci. Geomech. Abstr. 40, 25–40.

Hakami, E. (1992): Joint aperture measurements – an experimental technique. In: Proc., Fractured and Jointed Rock Masses. Lake Tahoe, California.

Hakami, E. (1995): Aperture distribution of rock fractures. Ph.D. thesis, Division of Engineering Geology, Department of Civil and Environmental Engineering, Royal Institute of Technology, Stockholm, Sweden.

Hakami, E., Barton, N. (1990): Aperture measurements and flow experiments using transparent replica of rock joints. In: Proc., Rock Joint, Loen, Norway.

Hakami, E., Larsson, E. (1996): Aperture measurements and flow experiments on a single natural fracture. Int. J. Rock Mech. Min. Sci. 33, 395–404.

Hans, J., Boulon, M. (2003): A new device for investigation the hydro-mechanical properties of rock joints. Int. J. Numer. Anal. Meth. Geomech. 27, 513–548.

Iwano, M., Einstein, H. H. (1993): Stochastic analysis of surface roughness, aperture and flow in a single fracture. In: Proc., EUROCK93, Lisbon, Portugal, pp 135–141.

Iwano, M., Einstein, H. H. (1995): Laboratory experiments on geometric and hydromechanical characteristics of three different fractures in granodiorite. In: Proc., Eight International Congress on Rock Mechanics, vol. 2. Balkema, Rotterdam, 743–750.

Johns, R. A. (1991): Diffusion and dispersion of solute in a variable aperture fracture, Ph.D. Dissertation, Stanford University, Stanford, CA.

Keller, A. (1998): High resolution, non-destructive measurement and characterization of fracture apertures. Int. J. Rock Mech. Min. Sci. 35(8), 1037–1050.

Kulatilake, P. H. S. W., Shou, G., Huang, T. H., Morgan, R. M. (1995): New peak shear strength criteria for anisotropic rock joints. Int. J. Rock Mech. Min. Sci. Geomech. Abstr. 32, 673–697.

Kumar, A. T., Majors, A. P., Rossen, W. (1997): Measurements of aperture and multiphase flow in fractures with NMR imaging. SPE Form. Eval., 101–107.

Lanaro, F. (2000): A random field model for surface roughness and aperture of rock fractures. Int. J. Rock Mech. Min. Sci. Geomech. Abstr. 37, 1195–1210.

Lee, H. S., Cho, T. F. (2002): Hydraulic characteristics of rough fractures in linear flow under normal and shear load. Rock Mech. Rock Engng. 35(4), 299–318.

Mitani, Y., Esaki, T., Zhou, G., Nakashima, Y. (2003): Experiments and simulation of Shear – Flow Coupling properties of rock joint. In: Proc., 39th Rock mechanics conference: Glückauf, Essen, 1459–1464.

Mitani, Y., Esaki, T., Sharifzadeh, M., Vallier, F. (2003): Shear – Flow coupling properties of rock joint and its modeling Geographical Information System (GIS). In: Proc., 10th ISRM Conference, South African Institute of Mining and Metallurgy, 829–832.

Ohtani, T., Nakashima, Y., Nakano, T., Muraoka, H. (2000): X-ray CT imaging of pores and fractures in the Kakkonda granite, NE Japan. In: Proc., World Geothermal Congress, Kyushu – Tohoku, Japan, 1521–1526.

Pyrak-Nolte, L. J., Myer, L. A., Cook, N. G., Witherspoon, P. A. (1987): Hydraulic and mechanical properties of natural fractures in low permeability rock. In: Proc., Sixth International Congress on Rock Mechanics. Montreal, Canada, 225–231.

Seidel, J. P., Haberfield, C. M. (2002): A theoretical model for rock joints subjected to constant normal stiffness and direct shear. Int. J. Rock Mech. Min. Sci. 39, 539–553.

Sharifzadeh, M. (2005): Experimental and theoretical research on hydromechanical coupling properties of rock joint. Ph.D. thesis, Kyushu University, Japan, 226.

Sharifzadeh, M., Mitani, Y., Esaki, T., Urakawa, F. (2004a): An investigation of joint aperture distribution using surface asperities measurement and GIS data processing. Asian Rock Mechanics Symposium (ARMS3), Mill Press, Kyoto, 165–171.

Sharifzadeh, M., Mitani, Y., Esaki, T., Urakawa, F. (2004b): Determination of evaluation method of rock joint aperture distribution. EUROCK2004, Salzburg, Austria, Balkema, Rotterdam, 505–568.

Stephanie, P., Bertels, D., DiCarlo, A., Blunt, M. J. (2001): Measurement of aperture distribution, capillary pressure, relative permeability, and in situ saturation in a rock fracture using computed tomography scanning. Water Resour. Res. 37(3), 649–662.

Tse, R., Cruden, D. M. (1979): Estimating joint roughness coefficient. Int. J. Rock Mech. Min. Sci. Geomech. Abstr. 16, 303–307.

Xie, H. P., Wang, J. A., Xie, W. H. (1997): Fractal effects of surface roughness on the mechanical behavior of rock joints. Chaos Solutions Fractals 8, 221–252.

Author's address: Mostafa Sharifzadeh, Department of Mining, Metallurgy and Petroleum Engineering, Amirkabir University of Technology, Hafez 424, Tehran 15875-4413, Iran; e-mail: sharifzadeh@aut.ac.ir